

# A modular reactor to simulate biofilm development in orthopedic materials

Joana Barros,<sup>1,2,4\*</sup> Liliana Grenho,<sup>1,2</sup> Cândida M. Manuel,<sup>4,5</sup> Carla Ferreira,<sup>4</sup>  
Luís F. Melo,<sup>4</sup> Olga C. Nunes,<sup>4</sup> Fernando J. Monteiro,<sup>1,2</sup> Maria P. Ferraz<sup>1,2,3</sup>

<sup>1</sup>INEB-Instituto de Engenharia Biomédica, Portugal. <sup>2</sup>FEUP-Faculdade de Engenharia, Universidade do Porto, Departamento de Engenharia Metalúrgica e Materiais, Portugal. <sup>3</sup>CEBIMED-Centro de Estudos em Biomedicina, Universidade Fernando Pessoa, Portugal. <sup>4</sup>LEPABE-Laboratory for Process Engineering, Environment, Biotechnology and Energy, Dept. Chemical Engineering, University of Porto, Portugal. <sup>5</sup>ULP-Universidade Lusófona do Porto, Portugal

Received 17 August 2013 · Accepted 1 October 2013

**Summary.** Surfaces of medical implants are generally designed to encourage soft- and/or hard-tissue adherence, eventually leading to tissue- or osseo-integration. Unfortunately, this feature may also encourage bacterial adhesion and biofilm formation. To understand the mechanisms of bone tissue infection associated with contaminated biomaterials, a detailed understanding of bacterial adhesion and subsequent biofilm formation on biomaterial surfaces is needed. In this study, a continuous-flow modular reactor composed of several modular units placed in parallel was designed to evaluate the activity of circulating bacterial suspensions and thus their predilection for biofilm formation during 72 h of incubation. Hydroxyapatite discs were placed in each modular unit and then removed at fixed times to quantify biofilm accumulation. Biofilm formation on each replicate of material, unchanged in structure, morphology, or cell density, was reproducibly observed. The modular reactor therefore proved to be a useful tool for following mature biofilm formation on different surfaces and under conditions similar to those prevailing near human-bone implants. [Int Microbiol 2013; 16(3):191-198]

**Keywords:** orthopedic materials · orthopedic conditions · modular reactors · continuous flow · biomaterials · biofilm formation

## Introduction

Biofilm-related infections associated with indwelling medical devices, such as orthopedic implants and prostheses, have become a major clinical concern and reflect the failed attempts to prevent their formation and to treat affected patients [31]. In fact, bone-tissue and prosthetic-joint infections are among the worst complications in orthopedic surgery and traumatol-

ogy and may lead to the complete failure of the arthroplasty, amputation, prolonged hospitalization, and even death [4,9,27].

Bacterial attachment to biomaterial surfaces is an important step in the pathogenesis of these infections. Their exact mechanism remains unclear but several studies have been directed at better understanding the development, structure, and impact of bacterial biofilms associated with indwelling medical devices. A large proportion of implant-related infections is caused by *Staphylococcus aureus*, *S. epidermidis*, and *Escherichia coli* [1,18,27]. The pathogenicity of biofilm-dwelling *S. epidermidis* has at least in part been attributed to the development of extracellular polymeric substances (EPS) [18,27,30] that protect the bacterial population against host defense mechanisms and antimicrobial agents [1,27].

\*Corresponding author: J. Barros

INEB-Instituto de Engenharia Biomédica  
Universidade do Porto  
Rua do Campo Alegre, 823  
4150-180 Porto, Portugal  
Phone: +351-226074900  
E-mail: joanabarro@fe.up.pt

Hydroxyapatite (HA) has exceptional biocompatibility and bioactivity with respect to bone cells and tissues, probably because of its similarity to the hard tissues of the body [11]. It has therefore been extensively used as a coating for orthopedic implants or as a bone substitute. Bone contains natural HA crystals with needle-like and rod-like shapes well-arranged within a polymeric matrix of collagen type I. Nanophased HA is able to bind bone and to interact with macromolecules that participate in the preliminary events leading to bone bonding and tissue regeneration [10]. However, the introduction of nanophased HA materials into the body is always associated with the risk of microbial infection, particularly in the fixation of open-fractures and in joint-revision surgeries [27]. Consequently, these implanted materials represent sites of weakness for host defenses such that they allow the attachment even of bacteria with a low level of virulence [16].

The most promising strategies for preventing orthopedic infections seek to inhibit bacterial adhesion prior to biofilm formation, especially during the initial 6 h following implantation [9,10], the critical phase in the occurrence of device-associated infections [9]. To achieve this goal requires a detailed understanding and quantification of the events that occur during initial bacterial adhesion and subsequent biofilm formation on biomaterial surfaces.

One way to reproducibly study and visualize biofilms and cellular attachment is to use biofilm reactors [6]. During the last several decades, attempts have been made to develop laboratory biofilm reactors that minimize the heterogeneity of experimental conditions in order to simplify the analysis and validation of biofilm data and to enable direct and real-time assessment of the bacterial colonization of submerged surfaces [6,13,14,22,23,30]. Biofilm reactors present several advantages with respect to the definition and control of hydrodynamic parameters such as flow velocity, Reynolds number, and shear stress [22]. Moreover, properly designed biofilm reactors contribute to minimizing experimental problems associated with inconsistent and ill-defined rinsing of “reversibly” bound cells, the variability of culture media, radiolabeled substrates, or vital stains, and the exposure of biofilm to medium-air interfacial forces [22]. Two of the best known types of reactors for the open continuous culture of biofilms are annular reactors (Rotatorque) and the Robbins device [14,23]. However, while both operate as continuous-flow systems and contain fixed biofilm supports that can be easily removed for sampling, removal is only possible after the flow has been stopped, with the flow restarted by again closing the system [15,21]. Thus, the hydrodynamics are, in general, not similar to the conditions found near human bones in the body.

Additionally, in the Rotatorque reactor, fluid dynamics are not uniform throughout the system, leading to non-ideal mixing and non-uniform biofilm formation [17].

In this work, an in vitro model modular reactor was designed that replicates the conditions in the vicinity of living bone, including low flow rates, physiological body temperature, darkness, and low oxygen and nutrient levels. It also allows visual surveillance of bacterial adhesion and biofilm formation on biomaterial surfaces, easy manipulation and control of the environmental conditions, and periodic sampling and analysis with minimal disturbance of the biofilm samples.

## Materials and methods

**Preparation of nanohydroxyapatite and microhydroxyapatite samples.** Commercial nanohydroxyapatite (nanoHA) and microhydroxyapatite (microHA) provided as powders were kindly supplied by Fluidinova SA-Portugal (nanoXIM\_HAp202) and Plasma Biotall-UK (P218), respectively. The samples consisted of cylindrical nanoHA and microHA discs 10 mm in diameter that were prepared from 0.150 g of dry powder under a uniaxial compression stress of 8 MPa (Mestra Snow P3). All experimental conditions related to the compression and sintering procedure were previously published [2,20,24]. Briefly, three different sintering temperatures were used according to the material: 830 °C (nanoHA830) and 1000 °C (nanoHA1000), with a 15-min plateau and applying a heating rate of 20 °C/min, and 1300 °C (microHA1300), with a 1-h plateau and applying a heating rate of 20 °C/min followed by cooling to room temperature inside the oven. The samples were sterilized by two passages in 70 % ethanol during 15 min followed by a double washing in sterile physiological saline (0.9 % NaCl).

**Modular reactor set-up.** A transparent Perspex (polymethylmethacrylate), modular reactor containing 27 sampling discs (nanoHA830, nanoHA1000, and microHA1300) was randomly placed in each well (Figs. 1,2). This reactor was connected to a closed Pyrex vessel containing the bacterial culture, which was supplied to the reactor at a continuous flow rate of  $1.54 \times 10^{-8}$  m<sup>3</sup>/s and an internal velocity of  $2.19 \times 10^{-5}$  m/s by means of a peristaltic pump (RS Amidata) working at 8 rpm. The complete experimental set-up was composed of modular units, a bacterial suspension vessel, a stir plate and magnetic stirrer, a waste vessel, and the circulation tubes (Fig. 1). Three modular units were used in parallel, one for each incubation time (24, 48, and 72 h), and the same conditions were maintained in all of the modular units. This system was operated as “once-through”, i.e., discarding the effluent. The entire reactor was placed inside an incubator to achieve and maintain a temperature of approximately 37 °C, with agitation of the suspension vessel throughout the experiment. All components of the modular reactor were sterilized in an autoclave except for the modular reactor itself, which was sterilized in a 15 % sodium hypochlorite solution and then rinsed with sterilized water under aseptic conditions.

**Bacterial strain and culture conditions.** *Staphylococcus epidermidis* strain RP62A (ATCC 35984), a slime producer [3,6], was used to produce a monospecies biofilm in all experiments in this report. A plate count agar culture of the test strain not older than 2 days was incubated in 15 ml of tryptic soy broth (TSB) for 24 (±2) h at 37 °C with agitation at 150 rpm by an orbital shaker (Certomat HK, B. Braun Biotech, Göttingen, Germany). An aliquot of 200 µl was transferred to 600 ml of fresh TSB, and the cells were

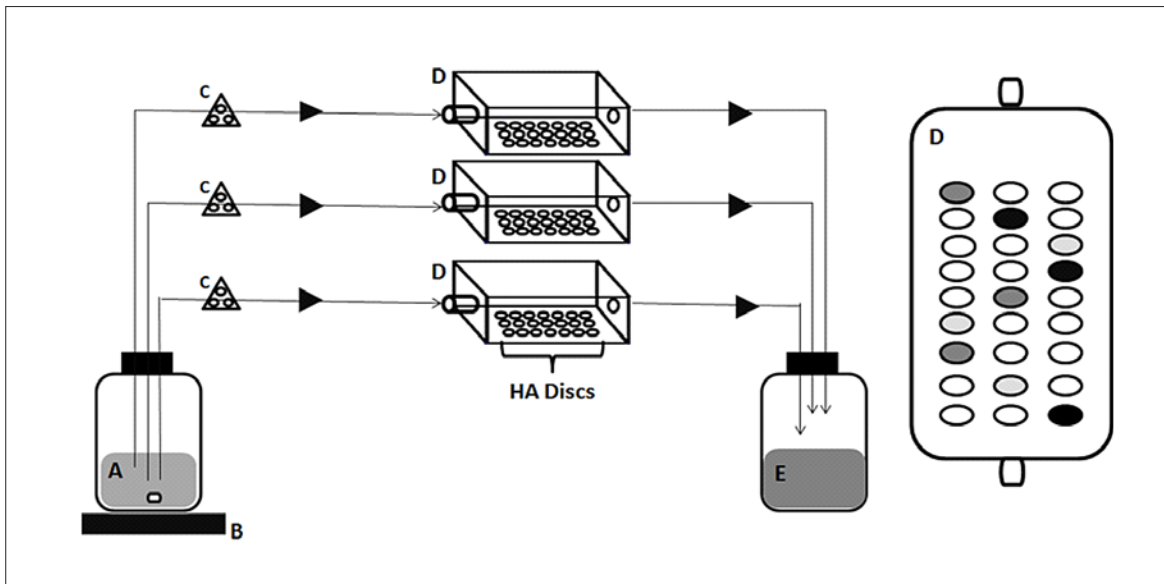


**Fig. 1.** Scheme of the experimental system used to obtain biofilm formation in the modular reactors. (A) Bacterial suspension vessel (5 l). (B) Magnetic stirrer. (C) Peristaltic pumps, 8 rpm. (D) Modular reactors to collect samples at 24, 48, and 72 h. A scheme of the HA discs randomly positioned in the reactor is also given; each color represents a different surface biomaterial. (E) Waste vessel.

allowed to grow for 18 ( $\pm$ 2) h, at 37 °C and 150 rpm, until they reached the exponential phase of growth. The inoculum was then transferred to the reactor suspension vessel in a volume of 10 % of the reactor’s useful volume (bacterial suspension containing approximately  $1 \times 10^8$  cells/ml).

**Biofilm formation on nanohydroxyapatite and microhydroxyapatite discs.** *Staphylococcus epidermidis* RP62A biofilm formation on the biomaterial discs was assessed over time. The sterile material samples were placed inside the modular reactor, which was operated under the above-described conditions. At 24, 48, and 72 h of incubation, the respective modular reactor was closed and the discs were collected, gently washed with sterile physiological saline (0.9 % NaCl), immersed in a flask containing 25 ml of sterile 0.9 % NaCl, and sonicated for 45 min in an ultrasonic bath (70 W, 35 kHz, Transsonic 420 ELMA) to release the attached bacteria into the suspension. The sonication time had been properly optimized in a preliminary study

(data not shown). The total numbers of metabolically active and cultivable cells were determined to assess biofilm formation. The structure of the biofilm was visualized by scanning electron microscopy (SEM). Nine discs of each biomaterial were used and all experiments were performed in triplicate.

**Total cell numbers.** The total number of cells in the diluted biofilm suspensions was determined by staining with 4',6-diamidino-2-phenylindole (DAPI, Merck, D9542), closely following a previously reported method [2]. The averages and standard deviations of the density of the biofilm samples were adjusted to the disc area.

**Metabolically active cell numbers.** The redox dye 5-cyano-2,3-ditolyl tetrazolium chloride (CTC) was used for direct epifluorescence microscopy counting of metabolically active bacteria [7] in dispersed biofilm samples. A 50 mM stock solution of CTC was prepared, filtered through a

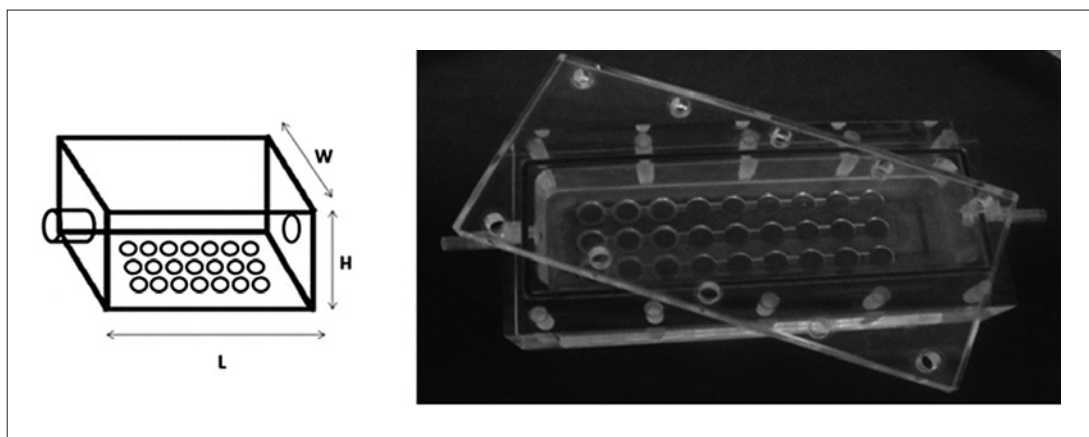


**Fig. 2.** Scheme and image of the modular reactor. (L) length (0.127 m); (H) height (0.018 m), (W) width (0.039 m).

0.22- $\mu\text{m}$  membrane, and stored in the dark at 4 °C. For each sample, 200  $\mu\text{l}$  of the biofilm suspension was collected and incubated in 4 mM CTC for 2 h in the dark at 37 °C with shaking at 130 rpm. The stained suspension was then filtered through a 0.22- $\mu\text{m}$  black polycarbonate membrane and the metabolically active bacteria were examined using an epifluorescence microscope with filter cube N2.1, since CTC excitation and emission occur at 450 and 630 nm, respectively. The averages and standard deviations of the biofilm density were calculated per unit surface area of the disc.

**Cultivable cell numbers.** The heterotrophic plate count is a procedure for estimating the number of colony-forming units (CFU) corresponding to cultivable bacteria. The method used in this study closely followed one previously reported [2]. The averages and standard deviations of the biofilm samples density were adjusted to the disc area.

**Scanning electron microscopy (SEM).** The methods for SEM observation and sample preparation closely followed those previously reported [2]. Five fields for each sample were randomly chosen to eliminate the possible uneven distribution of bacteria. Magnification was between 1000 and 15,000 $\times$ ; when required, higher magnifications were used to assess bacterial biofilm morphology and the interactions between the bacteria and the material surfaces.

**Statistical analysis.** The results of all the biofilm assays were compared using one-way analysis of variance (ANOVA), followed by post-hoc comparisons for all possible combinations of group means by applying the Tukey HSD multiple comparison test using SPSSV Statistics (vs.19.0, Chicago). In all cases,  $P < 0.05$  denoted significance.

## Results

The modular reactor and experimental set up described in Materials and methods (Figs. 1,2) was tested in several experiments to confirm use of this system to monitor changes in the growth and accumulation of a biofilm under conditions of a laminar flow rate ( $1.54 \times 10^{-8} \text{ m}^3/\text{s}$ ), low shear stress ( $2.26 \times 10^{-1} \text{ N/m}^2$ ), and low velocity ( $2.19 \times 10^{-5} \text{ m/s}$ ). The reactor internal dimensions were  $L = 0.127 \text{ m}$ ,  $H = 0.018 \text{ m}$ , and  $W = 0.039 \text{ m}$  (Fig. 2). The hydrodynamic variables were the hydraulic diameter ( $2.46 \times 10^{-2} \text{ m}$ ) and the cross-sectional area of the reactor ( $7.02 \times 10^{-4} \text{ m}^2$ ). The hydrodynamic flow near the biofilm samplings was positioned after the inlet stabilization zone ( $2.0 \times 10^{-2} \text{ m}$ ).

To verify whether the data obtained with the modular reactor were reproducible and therefore suitable for biofilm formation assays, the ability of *S. epidermidis* RP62A to form biofilms on different ceramic biomaterial discs (nanoHA830, nanoHA1000, and microHA1300) during up to 72 h of incubation was assessed. The results are shown in terms of total cell density (Fig. 3A), metabolically active cell density (Fig. 3B), and cultivable cell density (Fig. 3C). Biofilm structure and morphology were assessed by SEM at 72 h of incubation (Fig. 4).

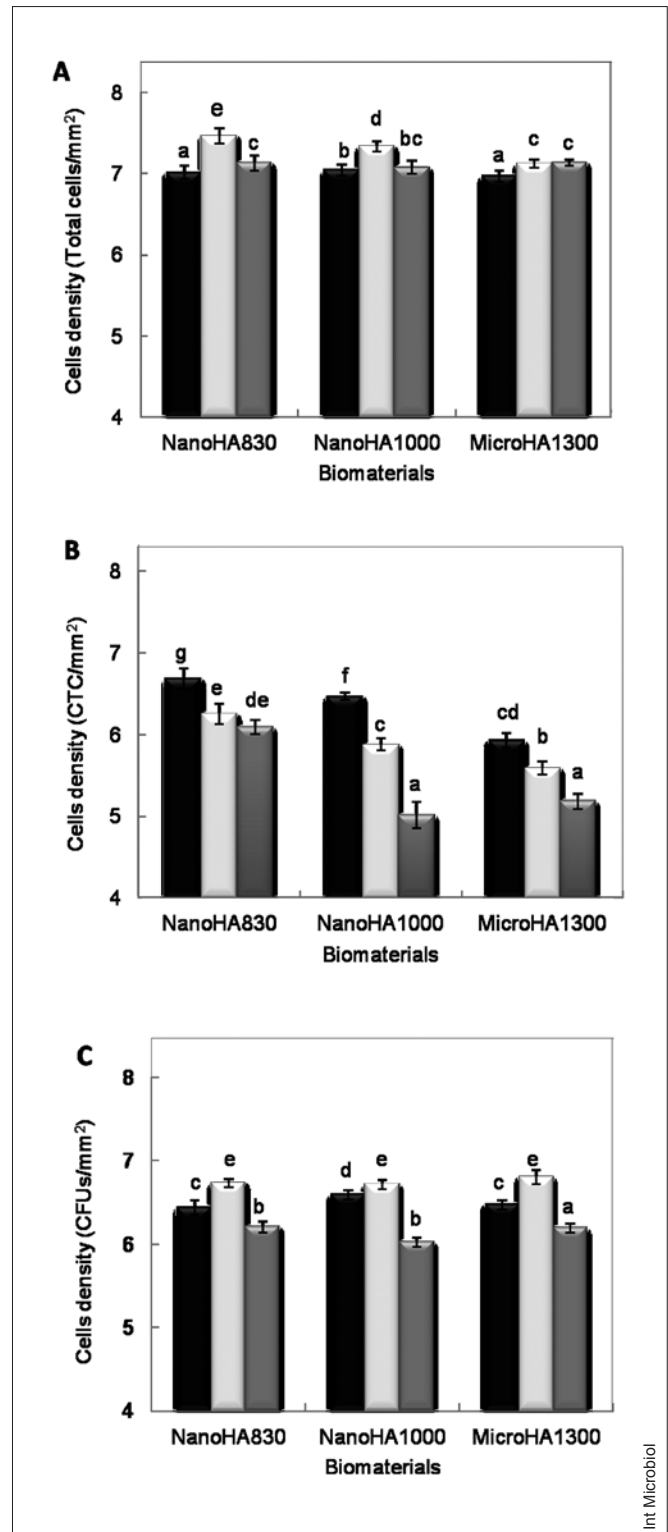


**Fig. 3.** Attached cells per unit surface area: total (A), metabolically active (B), and cultivable cells (C). The biofilms were grown on nanoHA and microHA discs in the modular reactor operated for 72 h. Different lowercase letters indicate significant differences ( $P < 0.05$ ) according to a Tukey HSD test. In black, 24 h; light grey, 48 h; and dark grey, 72 h

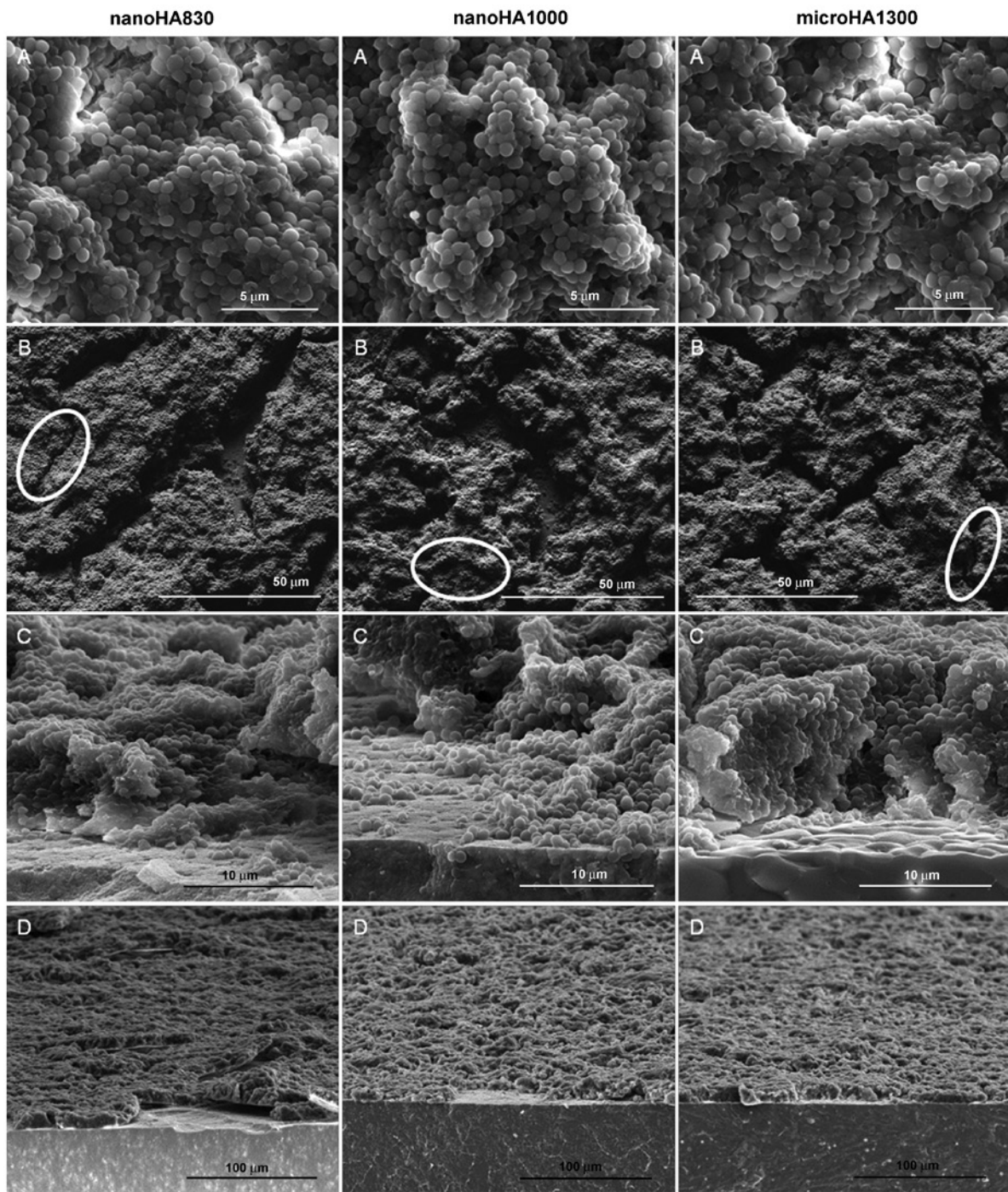


Fig. 4. SEM micrographs of biofilm growth on nanoHA and microHA discs at 72 h of incubation. The circles indicate the water channels.

Replicates of each biomaterial were placed in randomly chosen locations inside the reactor at 24, 48, and 72 h in order to check reproducibility. Since no significant differences were found among replicates of each biomaterial ( $P > 0.07$ ), it was concluded that the location of the sample inside the modular

unit, for each incubation time, did not affect the structure or the morphology of the biofilm nor the cell density.

In the *S. epidermidis* biofilms, similar profiles were obtained for total (Fig. 3A) and cultivable (Fig. 3C) cell density, with an increasing number of bacteria attaching to the bioma-

terials for up to 48 h. After this time point, the cell density of the biofilm decreased (Fig. 3A,B) except on microHA1300 discs, where the number of total adhered bacteria remained similar between 48 and 72 h of incubation ( $P > 0.05$ ) (Fig. 3A). The nanoHA830 discs had the highest and the microHA1300 discs the lowest total cell density up to 48 h [ $(3.01 \pm 0.65) \times 10^7$  total cells/mm<sup>2</sup> and  $(1.33 \pm 0.15) \times 10^7$  total cells/mm<sup>2</sup>, respectively] (Fig. 3A). After 48 h, the biofilms that had formed on the three biomaterials were similar ( $P > 0.05$ ) (Fig. 3A).

The data obtained for cultivable *Staphylococcus epidermidis* were also similar, nor were there significant differences ( $P > 0.05$ ) between the three biomaterials at 48 h (Fig. 3C). As with total cell numbers, after 48 h the highest number of cultivable cells occurred on the nanoHA830 discs [ $(1.61 \pm 0.22) \times 10^6$  CFU/mm<sup>2</sup>] and the lowest number on the microHA1300 discs [ $(1.06 \pm 0.13) \times 10^6$  CFU/mm<sup>2</sup>] (Fig. 3C).

The number of metabolically active cells (CTC-positive) decreased during 72 h of incubation (Fig. 2B). Again, the highest number of metabolically active cells was found on the nanoHA830 discs and the lowest number of on the microHA1300 discs (Fig. 3B).

As seen in the SEM images, mature biofilms had formed on the biomaterial surfaces after 72 h (Fig. 4) and their morphology and structure evidenced the production of extracellular polymeric substance (EPS) (Fig. 4A), three dimensional mushroom-like or pillar-like structures (Fig. 4C,D), and possibly water channels (Fig. 4B). In addition, the biofilms were seen to include multiple layers of bacterial cells (Fig. 4C,D) embedded in EPS (Fig. 4A).

## Discussion

A variety of laboratory-based model systems are available for the cultivation and study of biofilm communities. An important prerequisite of these systems is that they should simulate both the architecture and the spatial heterogeneity of the microbial community [19]. If the hydrodynamic pattern around the biofilm is overlooked, interpretations of the attachment and growth of microbial layers may be biased, because hydrodynamics directly affect shear stress and substrate mass transfer, and thus, in turn, biofilm development and architecture [28]. In this work, conditions closely mimicking those surrounding human bone, including hydrodynamic parameters such as flow rate and shear stress, were established to grow biofilms in the laboratory. Several studies [6,14,15,28] have shown that the hydrodynamic conditions determine the rate of bacterial transport as well as oxygen and nutrient diffusion to

the surface of the biofilm, thereby determining its structure. While developing the modular reactor, particular attention was paid to the hydrodynamic entry length, which is an important determinant in stabilizing the hydrodynamic flow and allowed comparisons between data obtained from different locations in the reactor. For rectangular ducts of aspect ratio (width/height)  $> 2$ , the entry length in laminar flow can be estimated by the following expression, adapted from Schetz and Fuhs [25]:

$$L_e = D_h(0.25 + 0.015 R_e)$$

where  $L_e$  is the entry length,  $D_h$  is the hydraulic diameter of the duct, and  $R_e$  the Reynolds number based on the hydraulic diameter [25]. In the present work, the entry length given by the above equation was around 0.001 m. Since the inlet conditions of the modular reactor did not exactly replicate those indicated by Schetz and Fuhs [25], the real entry length may have been somewhat higher but it was always less than a few millimeters, clearly within the reactor's inlet stabilization zone (0.02 m). In addition, others aspects were taken into consideration in the reactor's design, such as easy removal of the colonized substrata (the discs) without disturbing the biofilm formed in other zones of the modular reactors; the use of high-quality materials with high corrosion resistance, easy cleaning and sterilization; and the possibility of continuous macro- and microscopic monitoring. Given that one modular reactor was used for each period of incubation (24, 48, and 72 h), the colonization substrata were easily collected without disturbing the biofilm formed on the biomaterial surfaces of the other modular reactors. This kind of system is particularly suited for low flow rate experiments, namely, laminar flow (uniform and rectilinear stream lines), which better simulate orthopedic situations. Moreover it substantially reduces the cost of culture media preparation [29].

The results obtained with this reactor system are comparable to those already described by different authors using other experimental set ups. For example, similar total cell densities on different materials after 48 h were reported by Huang et al. [17], who grew *E. coli* biofilms in a parallel-plate flow cell reactor. The experiments of Shapiro et al. [26] were aimed at obtaining reproducible *S. epidermidis* RP62A biofilms on glass slides with the DFR system (Drip Flow Biofilm) and they established very low flow velocities such as in the present work. Those authors found that the mean number of viable bacteria in the biofilms increased until 48 h, with no significant differences occurring after this time among the different conditions. In another study, by Pereira et al. [23], in

which a flow cell reactor was used, the bacterial density on Perspex plates increased over time and the cultivable and total cell densities followed a similar pattern as in our system. Thus, although different morphological and chemical surface properties may affect the initial attachment, in the long term they do not seem to greatly affect the final build-up of the biofilm.

A decrease over time in the number of metabolically active cells (assessed in this study by CTC) was also recorded by Créach et al. [7], in their study of the growth of *E. coli* on M63 + 0.01 % D-glucose. One possible explanation for this reduction in cell numbers is the effect of EPS (see below), which in significant amounts tends to limit substrate penetration through the biological matrix.

Figure 4 shows the architecture of the relatively mature biofilm and substantial EPS production. The same indicators of a mature biofilm were noted by Williams et al. [31], who used a modified CDC (Center for Disease Control and Prevention, USA) biofilm reactor to develop mature biofilms of *S. aureus* on the surface of polyetheretherketone (PEEK). Well-established, mature biofilms reinforce bacterial resistance to antibiotics and influence the rate of genetic material exchange between microorganisms organized in these structures [5,8]. Thus, the reproduction of these biofilms in in vitro reactor models is clinically relevant in studying biofilm-related infections [15].

Molecular biology has allowed many new insights into biofilm development. Thus, it is now known that the *icaADBC* operon in *S. epidermidis* controls the production of polysaccharide intercellular adhesin (PIA) [12] and that this operon may in turn be controlled by oxygen levels [6]. Cotter et al. [6] reported that higher oxygen levels reduce biofilm formation via repression of the *icaADBC* operon and consequently reduce the production of PIA. In our study, the low oxygen levels may have contributed to the high production of PIA in the biofilms formed on all of the biomaterial surfaces. In the micrographs, the cracks observed in the biofilms may have formed because of shrinkage during dehydration processing. Similar artifacts were observed by Williams et al. [30] in the biofilm matrix of *S. epidermidis* ATCC 35984 grown using the CDC biofilm reactor.

The prevention of medical device contamination by biofilm formation remains a challenge. A promising strategy is the development of new surfaces containing two or more antibacterial agents differentially targeting the different microorganisms present in biofilms. The screening and assessment of this and other technical solutions require reliable laboratory-based systems that closely simulate physiological conditions and are easy to operate.

The modular reactor developed for this study proved to be useful in monitoring reproducible biofilm development under laboratory-controlled conditions. It allowed for periodic sampling by the removal of colonized discs without the need to stop the flow, thus minimizing the contamination risk and the disturbance of the biofilms forming on the other discs. In addition, together with off-line SEM observations, our reactor system provided information on the build-up of a mature biofilm (EPS production and the formation of three dimensional mushroom-like or pillar-like structures as well as water channels) on different biomaterials, under conditions similar to those that prevail in the vicinity of human-bone implants.

**Acknowledgements.** The authors acknowledge financial support for this work by a research grant to J. Barros from the FEDER funds through COMPETE and by FCT-Fundação para a Ciência e a Tecnologia in the framework of the project NanoBiofilm (PTDC/SAU-BMA/111233/2009). Also, the provision of nanoHA (nanoXIM) by FLUIDINOVA, SA (Maia-Portugal) is greatly acknowledged.

**Competing interest.** None declared.

## References

1. An YH, Friedman RJ (1997) Laboratory methods for studies of bacterial adhesion. *J Microbiol Methods* 30:141-152
2. Barros J, Grenho L, Manuel C, Ferreira C, Melo L, Nunes O, Monteiro F, Ferraz M (2013) Influence of nanohydroxyapatite surface properties on *Staphylococcus epidermidis* biofilm formation. *J Biomat Appl*. doi: 10.1177/0885328213507300
3. Cerca N, Pier GB, Vilanova M, Oliveira R, Azeredo J (2005) Quantitative analysis of adhesion and biofilm formation on hydrophilic and hydrophobic surfaces of clinical isolates of *Staphylococcus epidermidis*. *Res Microbiol* 156:506-514
4. Cheate MD (1991) The effect of chronic orthopedic infection on quality-of-life. *Orthop Clin North Am* 22:539-547
5. Costerton W, Veeh R, Shirtliff M, Pasmore M, Post C, Ehrlich G (2007) The application of biofilm science to the study and control of chronic bacterial infections. *J Clin Invest* 11:1466-1477
6. Cotter JJ, O'Gara JP, Stewart PS, Pitts B, Casey E (2010) Characterization of a modified rotating disk reactor for the cultivation of *Staphylococcus epidermidis* biofilm. *J Appl Microbiol* 109:2105-2117
7. Creach V, Baudoux AC, Bertru G, Rouzic BL (2003) Direct estimate of active bacteria: CTC use and limitations. *J Microbiol Methods* 52:19-28
8. Cvitkovitch DG (2001) Genetic competence and transformation in oral streptococci. *Crit Rev Oral Biol Med* 12:217-243
9. Darley ESR, MacGowan AP (2004) Antibiotic treatment of Gram-positive bone and joint infections. *J Antimicrob Chemother* 53:928-935
10. Ferraz MP, Mateus AY, Sousa JC, Monteiro FJ (2007) Nanohydroxyapatite microspheres as delivery system for antibiotics: Release kinetics, antimicrobial activity, and interaction with osteoblasts. *J Biomed Mater Res A* 81:994-1004
11. Ferraz MP, Monteiro FJ, Manuel CM (2004) Hydroxyapatite nanoparticles: A review of preparation methodologies. *J Appl Biomater Biomech* 2:74-80

12. Fey PD, Olson ME (2010) Current concepts in biofilm formation of *Staphylococcus epidermidis*. *Future Microbiol* 5:917-933
13. Gattlen J, Zinn M, Guimond S, Korner E, Amberg C, Mauclair L (2011) Biofilm formation by the yeast *Rhodotorula mucilaginosa*: process, repeatability and cell attachment in a continuous biofilm reactor. *Biofouling* 27:979-991
14. Gilmore BF, Hamill TM, Jones DS, Gorman SP (2010) Validation of the CDC biofilm reactor as a dynamic model for assessment of encrustation formation on urological device materials. *J Biomed Mater Res B Appl Biomater* 93:128-140
15. Goeres DM, Loetterle LR, Hamilton MA, Murga R, Kirby DW, Donlan RM (2005) Statistical assessment of a laboratory method for growing biofilms. *Microbiology* 151:757-762
16. Grenho L, Manso MC, Monteiro FJ, Ferraz MP (2012) Adhesion of *Staphylococcus aureus*, *Staphylococcus epidermidis*, and *Pseudomonas aeruginosa* onto nanohydroxyapatite as a bone regeneration material. *J Biomed Mater Res A* 100:1823-1830
17. Huang CT, Peretti SW, Bryers JD (1992) Use of flow cell reactors to quantify biofilm formation kinetics. *Biotechnol Tech* 6:193-198
18. Kajiyama S, Tsurumoto T, Osaki M, Yanagihara K, Shindo H (2009) Quantitative analysis of *Staphylococcus epidermidis* biofilm on the surface of biomaterial. *J Orthop Sci* 14:769-775
19. Lawrence JR, Swerhone GDW, Neu TR (2000) A simple rotating annular reactor for replicated biofilm studies. *J Microbiol Methods* 42:215-224
20. Lopes MA, Monteiro FJ, Santos JD, Serro AP, Saramago B (1999) Hydrophobicity, surface tension, and zeta potential measurements of glass-reinforced hydroxyapatite composites. *Biomed Mater Res A* 45:370-375
21. Manuel CM, Nunes OC, Melo LF (2007) Dynamics of drinking water biofilm in flow/non-flow conditions *Water Res* 41:551-562
22. Mittelman MW, Kohring LL, White DC (1992) Multipurpose laminar flow adhesion cells for the study of bacterial colonization and biofilm formation. *Biofouling* 6:39-51
23. Pereira MO, Morin P, Vieira MJ, Melo LF (2002) A versatile reactor for continuous monitoring of biofilm properties in laboratory and industrial conditions. *Letters Appl Microbiol* 34:22-26
24. Santos JD, Knowles JC, Reis RL, Monteiro FJ, Hastings GW (1994) Microstructural characterization of glass-reinforced hydroxyapatite composites. *Biomaterials* 15:5-10
25. Schetz JA, Fuhs AE (1999) Fundamentals of fluid mechanics. In: Schetz JA, Fuhs AE (eds) John Wiley, NY, USA.
26. Shapiro JA, Nguyen VL, Chamberlain NR (2011) Evidence for persisters in *Staphylococcus epidermidis* RP62A planktonic cultures and biofilms. *J Med Microbiol* 60:950-960
27. Simchi A, Tamjid E, Pishbin F, Boccaccini AR (2011) Recent progress in inorganic and composite coatings with bactericidal capability for orthopaedic applications. *Nanomedicine: NBM* 7:22-39
28. Simoes M, Pereira MO, Vieira MJ (2007) The role of hydrodynamic stress on the phenotypic characteristics of single and binary biofilms of *Pseudomonas fluorescens*. *Water Sci Technol* 55:437-445
29. Stoodley P, Hall-Stoodley L, Costerton B, et al. (2012) Biofilms, biomaterials, and device-related infections. In: Ratner BD, et al. (eds) *Biomaterials science: an introduction to materials in medicine*. 3rd ed. Elsevier, p. 565-583
30. Williams DL, Bloebaum RD (2010) Observing the biofilm matrix of *Staphylococcus epidermidis* ATCC 35984 grown using the CDC biofilm reactor. *Microsc Microanal* 16:143-152
31. Williams DL, Woodbury KL, Haymond BS, Parker AE, Bloebaum RD (2011) A modified CDC biofilm reactor to produce mature biofilms on the surface of PEEK membranes for an *in vivo* animal model application. *Curr Microbiol* 62:1657-1663